Biophysical Chemistry 144 (2009) 123–129

Contents lists available at ScienceDirect

Biophysical Chemistry

journal homepage: http://www.elsevier.com/locate/biophyschem

Evidence of α fluctuations in myoglobin's denaturation in the high temperature region: Average relaxation time from an Adam–Gibbs perspective

Luis Olivares-Quiroz [a,*], Leopoldo S. Garcia-Colin [b]

[a] Colegio de Ciencia y Tecnologia, Universidad Autonoma de la Ciudad de Mexico, Mexico
[b] Departamento de Fisica, Universidad Autonoma Metropolitana-Iztapalapa, Mexico

ARTICLE INFO

Article history:
Received 10 June 2009
Received in revised form 23 July 2009
Accepted 28 July 2009
Available online 3 August 2009

Keywords:
α-relaxations
Myoglobin thermal denaturation
Adam–Gibbs theory
Myoglobin hydration entropy
Configurational entropy

ABSTRACT

In this work, we derive an analytical expression for the relaxation time τ as a function of temperature T for myoglobin protein (Mb, PDB:1MBN) in the high temperature limit ($T > T_g = 200$ K). The method is based on a modified version of the Adam–Gibbs theory (AG theory) for the glass transition in supercooled liquids and an implementation of differential geometry techniques. This modified version of the AG theory takes into account that the entropic component in protein's denaturation has two major sources: a configurational contribution ΔS_c due to the unfolding of the highly ordered native state N and a hydration contribution ΔS^{hyd} arising from the exposure of non-polar residues to direct contact with solvent polar molecules. Our results show that the configurational contribution ΔS_c is temperature-independent and one order of magnitude smaller than its hydration counterpart ΔS^{hyd} in the temperature range considered. The profile obtained for $\log \tau(T)$ from $T = 200$ K to $T = 300$ K exhibits a non-Arrhenius behavior characteristic of α relaxation mechanisms in hydrated proteins and glassy systems. This result is in agreement with recent dielectric spectroscopy data obtained for hydrated myoglobin, where at least two fast relaxation processes in the high temperature limit have been observed. The connection between the relaxation process calculated here and the experimental results is outlined.

1. Protein's denaturation and the glass transition

In order to perform their biological function, proteins must fold into an ordered and flexible quasi-crystalline three dimensional structure known as the native state [1]. Albeit early studies on protein folding assigned a rigid structure to the native state, a modern review of the structure–function paradigm conceives native state as a highly dynamical and flexible structure capable not only of collective rotational motions but also of vibrational displacements at different time scales as neutron scattering and dielectric spectroscopy have recently revealed [2]. The large spectrum of rotational and vibrational motions displayed by aminoacid residues, covalent and hydrogen bonds contains a large amount of physical information to understand fundamental biological processes such as association and dissociation occurring inside and outside the cell. In addition to protein internal motions, there is a large evidence that suggests that protein function is also highly influenced by couplings between residues lying at protein's surface and water molecules present in the hydration shell [3,4]. According to this view, protein's biological functions are thus not only determined by internal motions (rotations and vibrations) but also by dynamical couplings between protein's residues and solvent's molecules. Dielectric spectroscopy identifies two types of fluctuations in hydrated proteins: α fluctuations which usually obey a Vogel–Fulcher–Tamman relationship, $\log \tau \sim DT_0/(T - T_0)$, and β fluctuations which normally follow an Arrhenius profile, $\log \tau \sim 1/T$ [5]. These fluctuations have their origin at different spatial scales. Whereas α fluctuations can be traced to dynamics existing in bulk water, β fluctuations are more characteristic of dynamic processes observed in confined geometries with highly restrictive orientational possibilities as it usually occurs in hydration shells [6].

Experimental evidence have consistently shown that hydrated proteins and supercooled liquids exhibit a set of common thermodynamic and kinetic features [7–12]. At temperatures near $T = 200$ K, hydrated proteins undergo a kinetic transition characterized by a change in the slope of the mean square displacement $\langle x^2(T) \rangle$ and the onset of an excess of vibrational modes at low frequencies (bosonic peak) [13–15]. Both characteristics are also observed in supercooled liquids entering the glassy regime [11,12]. In this case, a kinetic arrest in the liquid state gives rise to the amorphous solid phase known as the glassy state [16]. From a thermodynamic point of view, protein's denaturation and the glass transition in supercooled liquids also offer some interesting similarities. Microcalorimetry measurements associated to protein's denaturation show the existence of a resonant peak in the heat capacity C_p versus temperature T curve in a wide variety of physical conditions [17]. The passage from the liquid state to the glassy structure in liquids cooled below their crystallization temperatures is

* Corresponding author.
E-mail address: luis.olivares@uacm.edu.mx (L. Olivares-Quiroz).

0301-4622/$ – see front matter © 2009 Elsevier B.V. All rights reserved.
doi:10.1016/j.bpc.2009.07.005

also accompanied by C_p manifestations. Whereas for protein's denaturation C_p increases as the unfolding transition temperature is approached, for supercooled liquids C_p falls out to a value more similar to the crystalline structure [18].

Configurational entropy plays a fundamental role both in protein's dynamics and the glass transition and it is presumably one of the most important mechanisms that directs both processes [19,20]. As the liquid is cooled below its crystallization temperature T_m avoiding crystallization, it approaches a new temperature T_g where the glassy phase emerges. As $T \to T_m \to T_g$, the liquid experiences a volume reduction and a substantial slowing down of translational and rotational degrees of freedom. Both effects contribute to the large increase of viscosity observed macroscopically as $T \to T_g$ [21]. In kinetic terms, the supercooled liquid enters to a non ergodic phase since the time scales required to attain equilibrium become extremely large compared to the experimental range accessible. For practical purposes, the liquid becomes 'frozen' in a non-equilibrium state [22]. On a thermodynamic scale, volume reduction and freezing of degrees of motion imply a decrease of conformational possibilities accessible to the supercooled liquid. Since entropy S is ~ log Ω, with Ω the number of conformations, the passage to the glassy state must be necessarily accompanied by an entropy decrease.

In 1965, Adam and Gibbs proposed a statistical mechanics approach to describe the sudden increase of viscosity and the slowing down of the collective modes in supercooled liquids as $T \to T_g$ [23]. The Adam–Gibbs theory (AG theory) depicts the supercooled liquid as a set of J clusters with a distribution of sizes $\{z_1, z_2, \ldots z_j\}$, where z_k is the number of particles in the cluster k. As the liquid is cooled below T_m, the particles within each cluster do not have enough time to diffuse and thus remain trapped within these clusters, which act like 'kinetic cages'. The AG theory denominates these clusters cooperative rearrangement regions (CRRs) since global diffusion is hindered and only structural rearrangements within these regions are allowed. The large increase in diffusion time prevents the particles from one CRR move to another CRR and in such sense, each CRR can be considered as independent. In order to derive an expression for the probability w for a CRR undergoes a configurational transition at temperature T, the AG theory assumes there is a minimum size z^* required to contribute to the configurational entropy of the system. This assumption physically means that smaller CRRs are not expected to play a significant role in the conformational transition of the supercooled liquid and thus can be discarded in all statistical mechanics calculations. According to these considerations, the average relaxation time τ can be expressed in terms of the configurational entropy in the following form

$$\tau(T) = \tau_0 \exp\left(\frac{\Delta\mu(T)\Delta s_c^*(T)}{RT\Delta S^{\text{config}}(T)}\right) \tag{1}$$

where $\Delta\mu$ is the energy required to activate a configurational transition for the smallest cluster capable to undergo such transition, Δs_c^* is the corresponding entropy change and ΔS^{config} is the overall configurational entropy change of the transition given by the sum of the entropy changes coming from all clusters with a distribution of sizes $\{z_j\}$, R is the gas constant and τ_0 is a reference time.

Protein denaturation is even more complex in entropic terms. In this case, entropy contributions are twofold due to an interplay between configurational rearrangements inside the polypeptide chain and rearrangements occurring in the surrounding water molecules. The total entropy change upon unfolding can be written thus as $\Delta S^{\text{unfold}} = \Delta S_c + \Delta S^{\text{hyd}}$, where the first term represents the increase in the configurational space available to the polypeptide chain due to thermal denaturation and the second takes into account the decrease in the number of conformational possibilities of the water molecules in the hydration shell once the hydrophobic residues have been exposed [24]. The interplay between these effects, known as the hydrophobic effect has been recognized as the major driving force in protein's folding and unfolding, being responsible for at least 70% of the total energy changes involved in protein's interaction with water [25]. In addition, protein's denaturation and the glass transition display also observable C_p manifestations. In both cases, C_p shows a significant variation in the vicinity of the corresponding transition. For supercooled liquids entering the glassy state, C_p exhibits a pronounced drop of up 40% of its value at the liquid state [22]. Protein's denaturation is also accompanied by heat capacity resonant peaks at T_d, the temperature of thermal denaturation [17]. The specific location and details of the C_p resonant peak depend on the protein considered.

The existence of a common thermodynamic background between protein's denaturation and the glass transition in supercooled liquids suggests that an entropy based theory like the AG formalism may be used as a physical tool to explore relaxation processes in protein's denaturation. To achieve this goal, we propose a generalization of the standard AG theory to take into account both entropy terms of relevance in protein's denaturation and simultaneously an analytical method to calculate the configurational entropy contribution ΔS_c based on geometric considerations. In order to make a comparison with experimental results, we shall select as a target system a highly helical protein like myoglobin (PDB: 1MBN) whose native state is composed by eight α helices and no β structure [26,27]. The criterion used to select myoglobin as a probe system is based mainly on the absence of β structure in the native state, which enables the use of a simple differential geometry approach to discuss helix formation and denaturation. In its more general form, the method depicted in the following paragraphs can take into account not only the usual helix-coil transitions in peptides but also wider classes of transitions between other types of secondary structure like the typical β-sheet → random coil transition observed in amyloidogenic formation mechanisms [28].

The paper is organized as follows. Section 2 discuss the physical conditions for applicability of the AG theory in protein's denaturation and establishes the general framework of the AG theory in the case of protein's relaxation. Sections 3 and 4 present the central results of this paper. In Section 3, a general method for calculating the configurational entropy contribution ΔS_c for a helical chain is devised and it is applied to determine the relaxation time τ as function of temperature T. Section 4 provides a connection between theoretical and experimental parameters. A discussion in terms of recent dielectric spectroscopy data obtained for myoglobin's denaturation is also presented.

2. Adam–Gibbs formulation for hydrated protein's relaxation

In this work we shall focus our attention to such denaturation processes governed mainly by the hydrophobic effect. This is, where $T\Delta S^{\text{unfold}} \gg \Delta H^{\text{unfold}}$ holds. This assumption is necessary in order to consider an extension of the AG theory for protein's relaxation since AG theory is based fundamentally on entropy contributions. This is not particularly restrictive since most folding and unfolding mechanisms in hydrated proteins have a large entropy contribution as discussed in Section 1. According to this, the total entropy change upon denaturation can be written as $\Delta S^{\text{unfold}}(T) = \Delta S_c(T) + \Delta S^{\text{hyd}}(T)$, as previously discussed.

We shall identify the analogue of the CRRs in supercooled liquids as the structural units that integrate the secondary structure in globular proteins, this is, the α-helices and β-sheets. These structures are the natural choices for CRR since for small, single domain proteins they can fold and refold independently. With these considerations, the AG relaxation time for protein's denaturation can be written as,

$$\tau(T) = \tau_0 exp\left(\frac{\Delta\mu\Delta s_c^*}{RT(\Delta S_c(T) + \Delta S^{\text{hyd}}(T))}\right), \tag{2}$$

where Δs_c^* should be identified in this case with the configurational entropy change associated with the smallest secondary structure capable to undergo a configurational transition. In Eq. (2), ΔS_c must be understood as the entropy change due to the unfolding of the native state as a whole, which can contain in principle two types of contributions: one from α-helices's denaturation and other from β-sheets' denaturation. For a general case in which the native state is composed by n α-helices and m β-sheets with distribution of sizes $\{A_1, A_2, \cdots, A_n\}$ and $\{B_1, B_2, \cdots, B_m\}$, respectively, the total entropy contribution upon denaturation can be written simply as $\Delta S_c = \sum_{j=1}^{n} \Delta S_j^{\text{helix}} + \sum_{k=1}^{m} \Delta S_k^{\text{sheet}}$, where $\Delta S_j^{\text{helix}}$ is the entropy change of the j-th α helix and $\Delta S_k^{\text{sheet}}$ is the corresponding term for the k-th β unit.[1] Eq. (2) assumes thus the explicit form,

$$\tau(T) = \tau_0 exp\left(\frac{\Delta\mu\Delta s_c^*}{RT\left[\sum_{j=1}^{n} \Delta S_j^{\text{helix}}(T) + \sum_{k=1}^{m} \Delta S_k^{\text{sheet}}(T) + \Delta S^{\text{hyd}}(T)\right]}\right), \tag{3}$$

where, as mentioned before, no coupling between α helices and β sheets has been considered.

In this paper we shall apply Eq. (3) to describe the relaxation dynamics of a highly helical protein, discarding thus any contribution from β structures. For this, we shall consider thermal denaturation of hydrated myoglobin (Mb, PDB:1MBN) as our probe system. Mb is a protein conformed by a prosthetic heme group and $K=153$ residues integrated in a single polypeptide chain with molecular weight $M_w=$ 17,235 Da which folds into eight α-helices named from A to H [29,30]. Given that almost 80% of the native fold corresponds to α helical content [31], Mb's thermal denaturation can be considered in a good approximation as the unfolding of $n=8$ α-helices with a distribution of sizes $\{A_1, \cdots, A_8\}$, which range from $A_3=4$ aminoacid residues for the C-helix to $A_8=25$ aminoacid residues for the H-helix [32]. In regards to its native fold, Mb has a lack of β structure and disulphide bonds, thus thermal denaturation is reversible in a good approximation. In addition, Mb's denaturation has a significant entropic component as it has been shown by Makhatadze and Privalov [33,34]. Their estimation is that $T\Delta S^{\text{unfold}} > \Delta H^{\text{unfold}}$ at physiological temperatures, thus Eqs. (2) and (3) can be used to describe the entropic component of the average relaxation time. For a protein with no β structure like Mb, Eq. (3) can be simplified and reads,

$$\tau(T) = \tau_0 exp\left(\frac{\Delta\mu\Delta s_c^*}{RT\left[\sum_{j=1}^{n} \Delta S_j^{\text{helix}}(T) + \Delta S^{\text{hyd}}(T)\right]}\right). \tag{4}$$

which was obtained by setting $m=0$ in Eq. (3).

Eq. (4) represents the entropic contribution to the relaxation dynamics for a helical hydrated protein in the AG theory. Section 3 will be devoted to the explicit calculation of the entropic terms $\Delta S_c = \sum_{j=1}^{n} \Delta S_j^{\text{helix}}(T)$ and ΔS^{hyd} for myoglobin's denaturation.

3. Configurational and hydration entropies in myoglobin's denaturation

In order to calculate ΔS_c we proceed as follows. In a simplified picture, we shall represent Mb's native state as eight α helices with different sizes linked by an unstructured random coil. Along denaturation α-helices melt and therefore the denatured state D can be sketched in a first approximation by a single random coil. This assumption implies that any intermediate state I between N and D can be represented as a superposition of q helices with $0 \le q \le 8$ plus a small loop of aminoacid residues. Each state N, D or I has an internal energy E. This energy can be calculated in principle as the sum of the energy of the α helices existing in such state plus the energy of the random coil that links the corresponding helices. From this ansatz, the configurational partition function Q can be readily calculated in the weakly interacting limit as $Q=\sum_j \Gamma_j \exp(-\beta E_j)$, where Γ_j stands for the degeneracy of the energy level E_j and $\beta=(RT)^{-1}$ is the standard Boltzmann factor. The configurational entropy term ΔS_c follows from the relation

$$\Delta S_c = -\frac{1}{T}(\partial \log Q / \partial\beta) + R \log Q. \tag{5}$$

A word of caution regarding the internal energy E is appropriate. In general, E has two major components: a mechanical contribution arising from elastic deformations and a electrostatic contribution due to dipolar interactions, hydrogen bonds, van der Waals forces, etc.1 [35]. In this work, we focus our attention to mechanical and elastic contributions to the internal energy E and thus we neglect any electrostatic contribution to protein's stability. This is a working hypothesis and its validity will be reviewed and assessed in the final section.

An elastic polymer of length L can be represented as a three dimensional curve by the parametric equation $\boldsymbol{R}(\gamma)=[x(\gamma), y(\gamma), z(\gamma)]$, where (x, y, z) are the usual cartesian coordinates and γ is the arc's length of the curve. In this representation a straight line is defined by $\mathbf{T}=\mathbf{dR}/\mathbf{d}\gamma=\mathbf{a}$ with $\mathbf{a}$ a constant three dimensional vector. Then, the derivative of the tangent vector can be used as a parameter to measure the deviation of a particular curve from the straight line. Following the ideas proposed by Kamien et al. [36], Schlick et al. [37] and others, the elastic energy stored in a polypeptide chain of length L as a result of a deviation from the straight line is, at first order,

$$\varepsilon = A\int_0^L \left[\frac{d\mathbf{T}}{d\gamma}\right]^2 d\gamma, \tag{6}$$

where A is a constant that can be evaluated numerically for different chains and $\mathbf{T}$ is the tangent vector corresponding to the conformation C. In terms of the curvature $\kappa(\gamma) = \|\mathbf{T}'(\gamma)\|$, Eq. (6) can be re-written as,

$$\varepsilon = A\int_0^L \kappa^2(\gamma) d\gamma, \tag{7}$$

which is a general expression for any one dimensional curve in R^3. As expected, Eq. (7) implies that a straight line with curvature $\kappa=0$ has an elastic energy $\varepsilon=0$.

For any helix, the curvature is independent of the arc length [38] and it can be expressed in terms of its radius r and the vertical distance p between two adjacent turns (pitch). This is

$$\kappa(r,p) = \frac{4\pi^2 r}{p^2 + 4\pi^2 r^2}. \tag{8}$$

Substitution of Eq. (8) in Eq. (7) and subsequent integration provides an expression for ε in terms of r, p, and L given by

$$\varepsilon = AL\kappa^2 = \frac{16AL\pi^4 r^2}{(4\pi^2 r^2 + p^2)^2}. \tag{9}$$

Eq. (9) gives an expression for the elastic energy stored in an helical conformation with geometric parameters r, p and L. Eqs. (8) and (9) predict that both κ and ε fall out to zero very quickly either when $r \to 0$ and p remains finite or when r remains finite and $p \to \infty$. This behavior corresponds to the same physical situation: a helix stretched sufficiently enough to transform it into a straight line with curvature zero. It is interesting to realize that in the degenerate case $p=0$, which corresponds to circle of radius r, Eqs. (8) and (9) reduce to $\kappa=1/r$ and $E_c=AL/r^2$.

The next step in ΔS_c calculation requires a model for Mb's denaturation and the corresponding information on the structure of

[1] In principle, there is no reason to assume that $\Delta S^{\text{helix}} = \Delta S^{\text{sheet}}$ and therefore they have to be treated separately.

each of the states involved upon denaturation. Both issues are not free from controversy [29,39–41]. Based on NMR spectroscopy, a four-state mechanism $N \rightarrow I_1 \rightarrow I_2 \rightarrow D$ has been suggested for apoMb where the I_1 state comprises the formation of the *A*, *G*, and *H* helices and the I_2 state is considered as a new stage in which the *B* segment is formed [42–44]. Since the I_1 and I_2 states differ only on the folding of the *B* segment, we shall consider a much simpler three state model with a single intermediate state *I* associated with the pH 4 molten globule state [45–47]. Such consideration lies on solid experimental evidence. Uzawa et al. have found that the intermediate state I_1 and the pH 4 molten globule state have almost the same helical content and the same helices folded [48]. With such considerations, our model for Mb's denaturation will consist on a three state transition $N \rightarrow I \rightarrow D$ where *I* is the pH 4 molten globule state. Then, the elastic energy of the denatured, intermediate and native states can be written as,

$$\begin{aligned} \varepsilon_D &= AL\langle\kappa\rangle^2 \\ \varepsilon_I &= A\left(\kappa_\alpha^2 \sum_{k=A,G,H} l_k + \langle\kappa\rangle^2 L'\right) \\ \varepsilon_N &= A\left(\kappa_\alpha^2 \sum_{k=A\rightarrow H} l_k + \langle\kappa\rangle^2 L''\right) \end{aligned} \tag{10}$$

where *L* is the length of the denatured state, *L′* the length of the random coil present in the intermediate state and *L″* the length of the unstructured loop that connects the eight helices in the native state. κ_α is the curvature of a α helix and $\langle\kappa\rangle$ is the average curvature corresponding to a random coil. In the *I* state, the sum runs over the *A*, *G*, and *H* segments whereas that in the *N* state the sum runs over the eight helices, from *A* to *H*. The constant *A* can be determined experimentally, as we will show in the next Section.

For weakly interacting helices, the configurational partition function *Q* can be written explicitly as

$$\begin{aligned} Q = \Gamma_D \exp\left[-\beta AL\langle\kappa\rangle^2\right] + \Gamma_I \exp\left[-\beta A\left(\kappa_\alpha^2 \sum_{k=A,G,H} l_k + \langle\kappa\rangle^2 L'\right)\right] + \\ + \Gamma_N \exp\left[-\beta A\left(\kappa_\alpha^2 \sum_{k=A\rightarrow H} l_k + \langle\kappa\rangle^2 L''\right)\right] \end{aligned} \tag{11}$$

from where the configurational entropy ΔS_c can be readily calculated. In next section, we provide a numerical evaluation of the different quantities appearing in Eq. (11) based on experimental and molecular dynamics results reported by other groups. Then, $\Delta S_c(T)$ is obtained numerically for myoglobin's denaturation. The hydration contribution ΔS^{hyd} will be extracted from microcalorimetry data reported in [33,34]. From these results, the relaxation time τ for myoglobin's denaturation will be obtained.

4. Results and discussion

Numerical evaluation of Eqs. (10) and (11) for myoglobin's denaturation can be carried out through results obtained recently from MD simulations of apomyoglobin (apoMb) and Mb mechanical unfolding. Force-induced unfolding simulations performed by Choi et al. using an harmonic force $F = -kr_{NC}$ to increase the distance r_{NC} between the *N* atom of the Val^1 residue and the *C* atom of the Gly^{153} residue show that a cooperative unfolding transition occurs at $F = 250$ pN and $r_{NC} = 150$ Å for an elastic constant $k = 10\ \mathrm{J\,mol^{-1}\,Å^{-2}}$ [49]. The potential energy $U = kr_{NC}^2/2$ corresponds to the energy stored within the chain as a result of elongations and compressions, thus it can be associated with the elastic energy $\varepsilon = AL\kappa_\alpha^2$ obtained in Eq. (9). This identification yields $A = kr_{NC}^2/2L\kappa_\alpha^2$, where r_{NC} is the end-to-end distance when the unfolding transition begins, κ_α is the curvature of the α-helix and L is the length of the polypeptide chain in its fully extended configuration. This relation enables a numerical estimation for the parameter *A* in Eq. (9) for the particular case of myoglobin's mechanical deformation if the curvature κ_α of an α helix is known. Our result in Eq. (8) fills this gap. For a typical α helix with $r = 3$ Å and $p = 5.4$ Å, $\kappa_\alpha = 0.30\ \mathrm{Å^{-1}}$. According to Choi et al., apoMb and Mb's fully extended conformation corresponds to $L = 460$ Å [49]. These values yield $A = 2.77 \times 10^3\ \mathrm{J\,Å\,mol^{-1}}$ for the, until now, unknown constant.

The lengths *L*, *L′* and *L″* can be evaluated as follows. In its fully extended conformation, $L = (3\ \text{Å /residue}) \times 153\ \text{residues} \simeq 460$ Å [49]. The molten globule *I* corresponds to the early fold of helices *A*, *G* and *H* linked by a non-helical segment of length *L′*. Since *A*, *G* and *H* segments are 14, 18 and 25 residues long, there are 96 aminoacid residues that do not take part in the formation of the helices *A*, *G* and *H*. Then *L′* can be estimated as $L' = (3\ \text{Å /residue}) \times 96\ \text{residues} = 288$ Å. With regards to the *N* state, only ~39 aminoacid residues are not in a helical conformation, thus $L'' = 117$ Å. The sums in Eq. (10) are given by $\sum_{k=A,G,H} l_k = 298.5$ Å and $\sum_{A\rightarrow H} l_k = 596.6$ Å. A word of caution is needed regarding the length of chains folded into helical conformations and into random coils. Random coils suspended in fluids can adopt more or less expanded conformations depending on the molecular interactions between the solvent and the chain. Random coils have not necessarily larger sizes than more ordered conformations like α or β structures and thus, the mathematical condition $\sum_{k=A,G,H} l_k + L' = L$ and $\sum_{k=A\rightarrow H} + L'' = L$ does not necessarily holds. The average curvature $\langle\kappa\rangle$ for a random coil can be estimated from its counterpart κ_α. Since a random coil has no preferred direction, we expect that in the average, its curvature is close to zero. Then $\langle\kappa\rangle = f\kappa_\alpha$ where f is an adimensional number $f \ll 1$. For $f = 0.1$, $\langle\kappa\rangle = 0.030\ \mathrm{Å^{-1}}$.

Substitution of these quantities in Eq. (10) yields $\varepsilon_D = 1.12\ \mathrm{kJ\ mol^{-1}}$, $\varepsilon_I = 75\ \mathrm{kJ\ mol^{-1}}$ and $\varepsilon_N = 149\ \mathrm{kJ\ mol^{-1}}$. The energy ε_D obtained for the denatured state lies within the order of magnitude of the energy of thermal fluctuation $RT \sim 2.5\ \mathrm{kJ\ mol^{-1}}$ at physiological temperatures. This implies that the *D* state is highly driven by thermal fluctuations. Indeed, it is known that random-coils' conformations show a high sensitivity to small temperature variations. Since ε_D is of the order of RT, a scenario of continuous deformations for the *D* state at physiological temperatures is expected. In terms of energy differences between *D*, *I* and *N* states, our results show that $\Delta_N^D E \simeq 148\ \mathrm{kJ\ mol^{-1}}$ and $\Delta_I^D E \simeq 74\ \mathrm{kJ\ mol^{-1}}$. The latter is in agreement with estimations provided by Miksovska et al. for the unfolding enthalpy $\Delta_I^N H \simeq 76\ \mathrm{kJ\ mol^{-1}}$ [50]. However, our result for $\Delta_D^N E$ differs from the one reported by Wittung for the unfolding enthalpy $\Delta_D^N H = [223\text{–}265]\ \mathrm{kJ\ mol^{-1}}$ [51]. Our value $\Delta_I^N E = 74\ \mathrm{kJ\ mol^{-1}}$ is much closer to the value reported by Jamin et al. $\Delta_D^I H = 125\ \mathrm{kJ\ mol^{-1}}$ [52]. In both cases, the difference between both results is of the order of a few H-bonds and it might be associated with the presence of some residual H-bonding in the experimental realization or with the lack of the electrostatic contribution in our model.

Degeneracies Γ_j can be evaluated from Zwanzig's model for polypeptide chain's conformations [53]. For a chain of *K* residues with an average number $\nu + 1$ of accessible conformations, the degeneracy Γ_j associated with the energy level E_j can be written in terms of the number α of residues with native contacts as,

$$\Gamma = \nu^{K-\alpha} \binom{K}{\alpha} \tag{12}$$

where $\binom{x}{y}$ is the binomial coefficient for *x* and *y* and $0 \le \alpha \le K$. In this work, we shall assume each aminoacid residue has in the average $\nu = 3$, which is the smaller non trivial number of possible configurations. For a *D* state with $k = 153$ aminoacid residues and no residual native structure, $\Gamma_D = 3^{153}\binom{153}{0} \simeq 1 \times 10^{73}$. The *I* and *N* states have both a random coil of length *L′* and *L″*. This gives $\Gamma_I = 6 \times 10^{45}$ and $\Gamma_N = 4 \times 10^{18}$.

Numerical evaluation of ΔS_c through Eq. (11) with the values considered above shows that ΔS_c has a constant value $\Delta S_c = 1396\ \mathrm{J\,mol^{-1}\,K^{-1}}$ in a temperature interval from $T = 273$ K to $T = 373$ K.

In normalized, per-residue units, this value corresponds to $\Delta S_{c,norm} = 9.12\,JK^{-1}mol^{-1}\,residue^{-1}$, which is in good agreement with the value $\Delta S_{c,norm} = 11.40\,JK^{-1}mol^{-1}residue^{-1}$ obtained very recently from CD measurements in helix-coil transitions [54] and with the value $\Delta S_{c,norm} = 7.60\,JK^{-1}mol^{-1}$ obtained for de novo designed helical peptides [55]. Suarez and Diaz have performed MD simulations of the helix-coil transition in α-helix triple bundles like collagen, obtaining a value $\Delta S_{c,norm} = 5.33\,JK^{-1}mol^{-1}residue^{-1}$, which is almost 40% smaller than ours [56]. Our value shows larger differences with the one reported by Thompson et al. [57], $\Delta S_{c,norm} = 20\,JK^{-1}mol^{-1}residue^{-1}$. In this case a difference of almost 50% is observed. Our value however is closer to $\Delta S_{c,norm} = 15\,JK^{-1}mol^{-1}residue^{-1}$ reported by Makhatadze and Privalov [58].

In a more fundamental level, our result shows that the configurational configurational entropy ΔS_c associated with conformational changes of the protein's backbone, is either temperature-independent or a very slightly varying function of T, as has been proposed in previous works [57,58]. In protein folding studies, it is customary to choose ΔS_c as temperature-independent with a value between 8 and $20\,JK^{-1}mol^{-1}residue^{-1}$ as a working hypothesis. In this work we have obtained this result as a consequence of both the geometric structure of the N, I and D states and a weak interaction hypothesis. To the authors' best knowledge, it is the first time an analytical formalism is proposed to validate the temperature independence of ΔS_c. The result obtained here, $\Delta S_{c,norm} = 9.12\,JK^{-1}mol^{-1}residue^{-1}$, can be used also to calculate the configurational entropy of the smallest unit capable to structural reorganizations Δs^* that appears in the modified AG theory (Eq. (2)). This region can be identified with the C or D segments which are 4–6 aminoacid residues long. Selecting the C segment as the smallest unit capable to fold, then Δs^* lies between 36.4 and $54.2\,JK^{-1}mol^{-1}$ which gives a remarkable agreement with ultra-fast H/D exchange measurements carried out by Uzawa et al. who suggest a value of $32\,JK^{-1}mol^{-1}$ [48].

To evaluate the hydration contribution ΔS^{hyd} we use microcalorimetry data reported by Makhatadzde and Privalov [33] reproduced in Table 1. ΔS^{hyd} is presented as a sum of individual contributions from aromatic, polar and aliphatic groups in myoglobin. As can be seen from Table 1, the aromatic aminoacid residues play a minor role in hydration effects. Its contribution is one order of magnitude smaller than its aliphatic and polar counterparts. Within the experimental temperature range considered, ΔS^{hyd} is an increasing function of T with values ranging from $-9.5\,kJ\,K^{-1}mol^{-1}$ at $T = 278$ K to $-5.8\,kJ\,K^{-1}mol^{-1}$ at $T = 398$ K. In absence of any additional consideration, experimental data set in Table 1 can be represented by a linear fit in terms of T, $\Delta S^{hyd} = a_1 + a_2 T$, with $a_1 = -18.09\,kJ\,K^{-1}mol^{-1}$ and $a_2 = 0.03\,kJ\,K^{-2}mol^{-1}$. Fig. 1 shows experimental data, the fitted curve $\Delta S^{hyd} = a_1 + a_2 T$ and the configurational part ΔS_c obtained previously which is temperature-independent. A linear profile for $\Delta S^{hyd}(T)$ has also been observed in MD simulations of small hydrophobic chains (~25 aminoacid residues long) [59], although the hydration contribution in this case is one order of magnitude smaller than for myoglobin's. From a thermodynamic point of view, a linear profile for ΔS^{hyd} is also consistent with the fact that the corresponding hydration free energy ΔG^{hyd} given by $\Delta S^{hyd} = -(\partial \Delta G^{hyd}/\partial T)$ must display a maximum value for a given temperature T^*.

Table 1
Hydration entropy data for aliphatic ΔS^{hyd}_{alp}, aromatic ΔS^{hyd}_{arm} and polar ΔS^{hyd}_{pol} residues for myoglobin reproduced according to microcalorimetry data by Privalov and Makhatadze [33].

	278 K	298 K	323 K	348 K	373 K	398 K
ΔS^{hyd}_{alp}	−5298	−4195	−2969	−1909	−973	−160
ΔS^{hyd}_{arm}	−782	−580	−362	−178	−22	113
ΔS^{hyd}_{pol}	−3514	−4060	−4616	−5080	−5483	−5824
ΔS^{hyd}	−9594	−8835	−7947	−7167	−6478	−5871

The hydration effects for each group are assumed to be proportional to the water accessible surface area for each group times the normalized per square angstrom hydration enthalpy. All ΔS data are given in $J\,K^{-1}mol^{-1}$ units.

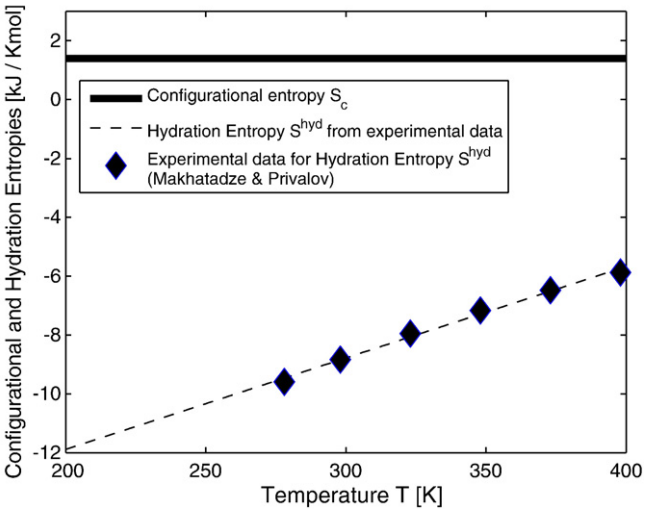

Fig. 1. Configurational and hydration entropies as function of temperature T. ΔS_c is temperature-independent for the temperature range considered. In normalized units, this corresponds to $\Delta S_{c,norm} = 9.12\,JK^{-1}mol^{-1}residue^{-1}$ (thick black line). Hydration contribution ΔS^{hyd} was obtained from a linear fit for experimental data [33] (Black diamonds). A linear fit $\Delta S^{hyd} = a_1 + a_2 T$ is carried out with $a_1 = -18.09\,kJ\,K^{-1}mol^{-1}$ and $a_2 = 0.03\,kJ\,K^{-2}mol^{-1}$ (Dashed line). The extrapolation of the linear behavior of ΔS^{hyd} was only considered up to $T = 200$ Kelvin, in the vicinity of the so-called dynamical transition in hydrated proteins which for hydrated myoglobin is assumed to occur between $T = 180$ K and 200 K. For temperatures below $T = 200$ K the hydration contribution may depart from the linear behavior observed at higher temperatures.

The relaxation time $\tau(T)$ can be written as,

$$\tau(T) = \tau_0 \exp\left(\frac{\Delta\mu\Delta s_c^*}{RT(a_1 + a_2 T + \Delta S_c)}\right), \tag{13}$$

with $\Delta s_c^* = 36.4\,JK^{-1}mol^{-1}$, $\Delta s_c = 1.4\,kJ\,K^{-1}mol^{-1}$, $a_1 = -18.09 kJ\,K^{-1}mol^{-1}$ and $a_2 = 0.03\,kJ\,K^{-2}mol^{-1}$. The quantity $\Delta\mu$ can be estimated through the activation energy E_{act}, which has been measured recently for hydrated myoglobin by Jansson et al. [60]. They estimated that $0.41 < E_{act} < 0.81$ eV. Since $\Delta\mu\Delta s_c^*/R\Delta S_c \sim E_{act}/k_B$, $\Delta\mu \simeq 10^7\,J\,K^{-1}mol^{-1}$. Fig. 2 shows a plot of $\log\tau$ versus $1000/T$ according to Eq. (13) for temperatures between $T = 200$ K and $T = 270$ K, approximately. This temperature range corresponds to the 'high' temperature limit since the dynamical transition observed in hydrated proteins usually occurs at $T \sim 200$ K. In order to explore this temperature range and in the absence of experimental information for ΔS^{hyd} in this temperature range, an extrapolation of data reported in reference ([33]) was performed (Fig. 1). For temperatures above the dynamical transition temperature $T \geq 200$ K we expect that $\Delta S^{hyd}(T)$ retains its linear character. No other experimental evidence has been reported so far. However, this assumption will be properly reviewed when new experimental data is available. Fig. 2 shows that $\log\tau$ exhibits a non-Arrhenius dynamics characteristic of α fluctuations in glassy systems and hydrated proteins in the 'high' temperature limit. Such temperature range is usually considered as temperatures lying between the dynamical transition temperature $T = 200$ K up to physiological temperatures $T = 300$ K. Given this temperature range, α fluctuations are normally associated with collective motions of aminoacid residues within the native structure.

Recently, Jansson and coworkers reported evidence of at least four relaxation processes in hydrated myoglobin [60,61]. At least one of them is observed in the temperature regime from $T = 200$ K to $T \simeq 270$ K(Process II, see [60,61]) which also shows a non-Arrhenius dynamics as the one showed in Fig. 2. Process II and our result have similar temperature dependencies for $T = 200$ K to $T = 300$ K so it is a temptation to identify both as the same process. However, such identification should be worked

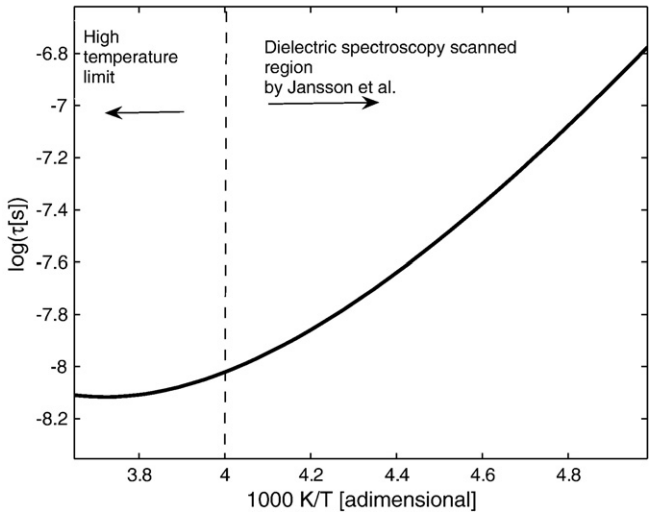

Fig. 2. Temperature dependence of the relaxation time $\log \tau$ for hydrated Mb obtained from Eq. (13) with $\tau_0 = 10^{-12}$ s, $\Delta\mu = 1\times10^{7}\,\mathrm{J\,K^{-1}\,mol^{-1}}$. The configurational ΔS_c and hydration ΔS^{hyd} contributions are obtained as discussed in Sections 2 and 3. The profile displayed by $\log \tau$ is non-Arrhenius as expected for α fluctuations for temperatures above the dynamical glass transition temperature $T = 200$ K. The plot has been divided in two regions. The temperature range explored experimentally by Jansson et al. [60] corresponds to temperatures below $T = 250$ K up $T = 140$ K (not shown here). Our result provides a theoretical prediction for $\log \tau$ for higher temperatures.

out with precaution. Process II spans over several orders of magnitude while $\tau(T)$ in Eq. (13) is a slower process. Nevertheless, additional experimental evidence suggest that Process II in myoglobin and other proteins is strongly related to global motions in polar aminoacid residues [62]. Since hydration contribution ΔS^{hyd} in myoglobin is dominated essentially by polar and aliphatic groups (see Table 1), it is plausible to consider that Eq. (13) captures appropriately the temperature dependence of Mb's relaxations in the high temperature limit.

In order to analyze the dependence of $\log \tau$ with respect to the type of transition proposed for Mb's denaturation, a two state transition $N \rightarrow D$ was considered by setting $\Gamma_I = 0$ in Eq. (11). In the weak interacting approximation used to calculate the configurational partition function Q (Eq. (11)), $\log \tau$ preserves its non-Arrhenius character whether a three or two state transition is considered. Both the two and three state transition model for Mb's denaturation predict that ΔS_c is temperature-independent in the range from $T = 200$K up $T = 300$ K with a small change around ~5% difference between numerical values for ΔS_c in the two and three state models. In both cases, the configurational term is one order of magnitude smaller than the hydration counterpart, thus at this level of approximation, the election of a two or three state model plays a minor role in the corresponding relaxation dynamics. A different temperature dependence for ΔS_c will likely arise when the weak interacting approximation is removed. In such case a modification of the temperature dependence of $\log \tau(T)$ is also expected.

5. Conclusions and final remarks

In this work we have presented a theoretical approach based on the AG theory and differential geometry to describe the temperature dependence of relaxation mechanisms in hydrated proteins. Specifically, we derived an analytical expression for $\log \tau$ as function of T for Mb, a protein selected by its high helical content. In the weak interacting approximation for the energies of the individual states, an analytical formula for the configurational entropy ΔS_c associated with the unfolding of the polypeptide chain was deduced. In this approximation, ΔS_c is shown to be temperature-independent with a value $\Delta S_{c,norm} = 9.12\,\mathrm{J\,K^{-1}\,mol^{-1}}$ residue^{-1}, in agreement with theoretical and experimental results published elsewhere and discussed along the work. The use of microcalorimetry data for the hydration contribution $\Delta S^{hyd}(T)$ enables us to provide a complete expression for $\log \tau$ as function of T in the temperature range from $T = 200$ K to $T = 300$ K. Our result shows that the hydration contribution ΔS^{hyd} is one order of magnitude larger than its configurational counterpart ΔS_c and therefore protein dynamics at this level is driven substantially by the hydration contribution, namely, by the structural reorganization of water molecules due to the exposure of myoglobin's aliphatic and aromatic groups. The non-Arrhenius dynamics obtained for $\log \tau$ is characteristic of the α fluctuations observed in the high temperature limit (temperatures above $T_g \simeq 200$ K) in hydrated proteins and glassy systems. The recent experimental observation of a fast relaxation dynamics in this temperature range with a similar non-Arrhenius profile suggests that the modified version of the AG theory presented in this work can account for the qualitative features observed in protein dynamics. It is worth to emphasize that the model presented here has only one adjustable parameter, the reference time τ_0. Other quantities like the free energy barrier $\Delta\mu$, the configurational entropy ΔS_c and its hydration counterpart ΔS^{hyd} have been determined using either experimental data or MD simulations according to discussions in Sections 3 and 4.

Determination of the energies E_j corresponding to the states N, I and D is performed taking into account only the mechanical energy stored in a flexible chain as a result of elongations and compressions. This point of view neglects the electrostatic contribution arising from H-bonding between polar aminoacid residues and water molecules. H-bonding plays a fundamental role in stabilizing native structures [63], [64] as H-bond formation between polaraminoacid residues and water molecules tends to decrease the free energy ΔG of the system by 50–80 kJ mol^{-1} [24]. However, at this level of approximation the introduction of the H-bond contribution would not change the temperature profile for $\log \tau$ significatively since the 'corrected' energies E_j^{elec} will correspond to just a shift from the mechanical counterpart. In order to include correctly the electrostatic contribution, the weak interacting approximation for the energy levels has to be modified. Our calculation have shown that in the high temperature region ($T > 200$ K), the relaxation process associated with structural rearrangements of polar and aliphatic residues exhibits a non-Arrhenius profile in agreement with experimental evidence reported elsewhere. These results work well in the high temperature region, where the hydration effects can be assumed not to deviate appreciably from the linear extrapolation here adopted (see Fig. 1). However, as T approaches the glass transition temperature, the linear profile for ΔS^{hyd} has to be seriously questioned. A detailed and complete analysis of $\log \tau$ for temperatures near the crossover T_g must necessarily modify the weak interacting approximation and include the H-bonding as an important feature.

Acknowledgments

L. Olivares-Quiroz acknowledges support from Sistema Nacional de Investigadores (SNI).

References

[1] K.A. Dill, S.B. Ozkan, T.R. Weikl, J.D. Chodera, V.A. Voelz, The protein folding problem: when will it be solved? Curr. Op. Struct. Biol. 17 (3) (2007) 342–346.
[2] J.A. McCammon, S.C. Harvey, Dynamics of Proteins and Nucleic Acids, Cambridge University Press, 1988.
[3] P.W. Fenimore, H. Frauenfelder, B.H. McMahon, F.G. Parak, Slaving: solvent fluctuations dominate protein dynamics and functions, Proc. Natl. Acad. Sci. U.S.A. 99 (25) (2002) 16047–16051.
[4] P.W. Fenimore, H. Frauenfelder, B.H. McMahon, R.D. Young, Bulk-solvent and hydration-shell fluctuations, similar to α and β fluctuations in glasses, control protein motions and functions, Proc. Natl. Acad. Sci U.S.A. 101 (40) (2004) 14408–14413.
[5] G. Chen, P.W. Fenimore, H. Frauenfelder, F. Mezei, J. Swenson, R.D. Young, Protein fluctuations explored by inelastic neutron scattering and dielectric relaxation spectroscopy, Philos. Mag. 88 (2008) 3877–3883.
[6] V. Lubchenko, P.G. Wolynes, H. Frauenfelder, Mosaic energy landscapes of liquids and the control of protein conformational dynamics by glass-forming solvents, J. Phys. Chem. B 109 (2005) 7488–7499.

[7] C.A. Angell, Formation of glasses from liquids and biopolymers, Science 267 (1995) 1924–1935.
[8] D. Wales, Energy Landscapes: Applications to Clusters, Biomolecules and Glasses, Cambridge University Press, 2004.
[9] L. Olivares-Quiroz, L.S. Garcia-Colin, Protein's unfolding and the glass transition: a common thermodynamic signature, AIP Conf. Proc. 978 (2008) 109–114.
[10] J. Fitter, T. Gutberlet, J. Katsaras (Eds.), Neutron Scattering in Biology: Techniques and Applications, Springer Verlag, Heidelberg, 2006.
[11] K.L. Nagai, S. Capaccioli, N. Shinyashiki, The protein "glass" transition and the role of the solvent, J. Phys. Chem. B 112 (2008) 3826–3832.
[12] A. Pacciaroni, S. Cinelli, G. Onori, Effect of the environment on the protein dynamical transition: a neutron scattering study, Biophys J. 83 (2002) 1157–1164.
[13] Y. Miyazaki, T. Matsuo, H. Suga, Low-temperature heat capacity and glassy behavior of lysozyme crystal, J. Phys. Chem. B 104 (2000) 8044–8052.
[14] K. Kawai, T. Suzuki, M. Oguni, Low-temperature glass-transitions of quenched and annealed bovine serum albumin aqueous solutions, Biophys J. 90 (10) (2006) 3732–3738.
[15] A.P. Sokolov, J.H. Roh, E. Mamontov, V.G. Sakai, Role of hydration water in dynamics of biological macromolecules, Chem. Phys. 345 (2008) 212–218.
[16] C.A. Angell, The old problems of glass and the glass transition and the many new twists, Proc. Natl. Acad. Sci. U.S.A. 92 (1995) 6675–6682.
[17] P.L. Privalov, A. I. Dragan, Microcalorimetry of biological macromolecules. Biophys. Chem. 126 (2007) 16–24.
[18] P.G. Debenedetti, F.H. Stillinger, Supercooled liquids and the glass transition, Nature 410 (2001) 259–267.
[19] H.B. Li, H.C. Wang, Y. Cao, D. Sharma, M. Wang, Configurational entropy modulates the mechanical stability of protein GB1, J. Mol. Biol. 379 (2008) 871–880.
[20] D.C. Sullivan, C.M. Lim, Configurational entropy of proteins: covariance matrix versus cumulative distribution calculations, J. Chinese Chem Soc. 51 (2004) 1209–1219.
[21] F.H. Stillinger, P.G. Debenedetti, Alternative view of self-diffusion and shear viscosity, J. Phys. Chem. B 109 (2005) 6604–6609.
[22] M.D. Ediger, C.A. Angell, S.R. Nagel, Supercooled liquids and glasses, J. Phys. Chem. 100 (1996) 13200–13212.
[23] G. Adam, J.H. Gibbs, On the temperature dependence of cooperative relaxation properties in glass-forming liquids, J. Chem. Phys. 43 (1) (1965) 139.
[24] A.V. Finkelstein, O.B. Ptitsyn, Protein Physics: A Course of Lectures, Academic Press Elsevier Science, 2002.
[25] N.T. Southall, K.A. Dill, A.D.J. Haymet, A view of the hydrophobic effect, J. Phys. Chem. B 106 (2002) 521–533.
[26] T. Suzuki, K. Imai, Evolution of myoglobin, Cell. Mol. Life Sci. 54 (1998) 979–1004.
[27] M. Brunori, D. Bourgeois, B. Vallone, Structural dynamics of myoglobin in Globins and other nitric oxide reactive proteins Part B. Book series Methods in Enzimology, Elsevier Academic Press 2008.
[28] M. Stefani, C.M. Dobson, Protein aggregation and aggregate toxicity: new insights into protein folding, misfolding diseases and biological evolution, J. Mol. Med 81 (2003) 678–699.
[29] H. Roder, Stepwise helix formation and chain compaction during protein folding, Proc. Natl. Acad. Sci. U.S.A. 101 (2004) 1793–1794.
[30] J.T.J. Lecomte, Y.H. Kao, M.J. Cocco, The native state of apomyoglobin described by proton NMR spectroscopy, Proteins 25 (1996) 267–285.
[31] H.C. Watson, The stereochemistry of the protein myoglobin, Prog. Stereochem. 4 (1969) 299.
[32] H.M. Berman, J. Westbrook, Z. Feng, G. Gilliland, T.N. Bhat, H. Weissig, I.N. Shindyalov, P.E. Bourne, The protein data bank, Nucleic Acids Res. 28 (2000) 235–242.
[33] G.I. Makhatadze, P.L. Privalov, Heat capacity of proteins 1: Partial molar heat capacity of individual aminoacid residues in aqueous solutions: hydration effects, J. Mol. Biol. 213 (1990) 375–384.
[34] G.I. Makhatadze, P.L. Privalov, Hydration effects in protein unfolding, Biophys. Chem. 51 (1994) 291–309.
[35] Y. Levy, J.N. Onuchic, Water and proteins: a love–hate relationship, Proc. Natl. Acad. Sci. U.S.A. (101) (2004) 3325–3326.
[36] R.D. Kamien, The geometry of soft materials: a primer, Rev. Mod. Phys. 74 (2002) 953–971.
[37] T. Schlick, Modeling superhelical DNA—recent analytical and dynamic approaches, Curr. Op. Struct. Biol. 5 (1995) 245–262.
[38] J.J. Stoker, Differential Geometry, Wiley InterScience, 1989.
[39] C. Nishimura, H.J. Dyson, P.E. Wright, The apomyoglobin pathway revisited: structural heterogeneity in the kinetic burst phase intermediate, J. Mol. Biol. 322 (2002) 483–489.
[40] D.J. Felitsky, M. Lietzow, P.E. Wright, Modeling transient collapsed states of an unfolded protein to provide insights into early folding events, Proc. Natl. Acad. Sci. U.S.A. 105 (2008) 6278–6283.
[41] M. Dametto, A.E. Cardenas, Computer simulations of the refolding of sperm whale apomyoglobin from high-temperature denatured state, J. Phjys. Chem. B 112 (2008) 9501–9506.
[42] D. Eliezer, J. Yao, H.J. Dyson, P.E. Wright, Structural and dynamic characterization of partially folded states of apomyoglobin and implications for protein folding, Nat. Struct. Biol. 5 (1998) 148–155.
[43] M. Jamin, The folding process of apomyoglobin, Protein Pept. Lett. 12 (2005) 229–234.
[44] C.H. Ramos, S. Weisbuch, M. Jamin, Diffusive motions control the folding and unfolding kinetics of the apomyoglobin pH 4 molten globule intermediate, Biochemistry 46 (2007) 4379–4389.
[45] Y.V. Griko, P.L. Privalov, S.Y. Venyaminov, V.P. Kutyshenko, Thermodynamic study of the apomyoglobin structure, J. Mol. Biol. 202 (1988) 127–138.
[46] E. Polverini, G. Cugini, F. Annoni, S. Abbruzetti, C. Viappiani, T. Gensch, Molten globule formation in apomyoglobin monitored by the fluorescent probe Nile Red, Biochemistry 45 (2006) 5111–5121.
[47] E. Bismuto, E. Di Maggio, S. Pleus, M. Sikor, C. Rocker, G.U. Nienhaus, D.C. Lamb, Molecular dynamics simulation of the acidic compact of apomyoglobin from yellowfin tuna, Proteins 74 (2009) 273–290.
[48] T. Uzawa, S. Akiyama, T. Kimura, S. Takahashi, K. Ishimori, I. Morishima, T. Fujisawa, Collapse and search dynamics of apomyoglobin folding revealed by submillisecond observations of alpha helical content and compactness, Proc. Natl. Acad. Sci. U.S.A. 101 (2004) 1171–1176.
[49] H.S. Choi, J. Huh, W.H. Jo, Similarity of force-induced unfolding of apomyoglobin to its chemical induced unfolding: an atomistic molecular dynamics simulation approach, Biophys. J. 85 (2003) 1492–1502.
[50] J. Miksovska, R.W. Larsen, Photothermal studies of pH induced unfolding of apomyoglobin, J. Protein Chem. 22 (2003) 387–394.
[51] P. Wittung-Stafshede, Effect of redox state on unfolding energetics of heme proteins, Biochim. Biophys. Act 1432 (1999) 401–405.
[52] M. Jamin, M. Antalik, S.N. Loh, D.W. Bolen, R.L. Baldwin, The unfolding enthalpy of the pH 4 molten globule of apomyoglobin measured by isothermal titration calorimetry, Protein Sci. 9 (2000) 1340–1346.
[53] R. Zwanzig, Simple-model of protein folding kinetics, Proc. Natl. Acad. Sci. U.S.A. 92 (1995) 9801–9804.
[54] A. Murza, J. Kubelka, Beyond the nearest-neighbor Zimm–Bragg model for helix-coil transition in peptides, Biopolymers 91 (2009) 120–131.
[55] R. Zhou, Trp-cage: folding free energy landscape in explicit water, Proc. Natl. Acad. Sci U.S.A. 100 (2003) 13280–13285.
[56] E. Suarez, N. Diaz, D. Suarez, Entropic control of the relative stability of triple-helical collagen peptide models, J. Phys. Chem. B 112 (2008) 15248–15255.
[57] J.B. Thompson, H.G. Hansma, P.K. Hansma, K.W. Plaxco, The backbone conformational entropy of protein folding: experimental measures from atomic force spectroscopy, J. Mol. Biol. 322 (2002) 645–652.
[58] G.I. Makhatadze, P.L. Privalov, On the entropy of protein folding, Protein Sci. 5 (1996) 507–510.
[59] M.V. Athawale, G. Goel, T. Ghosh, T.M. Trusket, S. Garde, Effects of lengthscales and attractions on the collapse of hydrophobic polymers in water, Proc. Natl. Acad. Sci U.S.A. 104 (2007) 733–738.
[60] H. Jansson, R. Bergman, J. Swenson, Relation between solvent and protein dynamics as studied by dielectric spectroscopy, J. Phys. Chem. B 109 (2005) 24134–24141.
[61] J. Swenson, H. Jansson, R. Bergman, Relaxation processes in supercooled confined water and implications for protein dynamics, Phys. Rev. Lett. 96 (2006) 247802.
[62] S. Bone, Time-domain reflectometry studies of water binding and structural flexibility in chymotrypsin, Biochim. Biophys. Act 916 (1987) 128–134.
[63] F. Despa, A. Fernandez, R.S. Berry, Dielectric modulation of biological water, Phys. Rev. Lett. 93 (2004) 228104.
[64] F. Despa, R.S. Berry, The origin of long-range attraction between hydrophobes and water, Biophys. J. 92 (2007) 373–378.